Ceramics International xxx (xxxx) xxx

Contents lists available at ScienceDirect

Ceramics International

journal homepage: www.elsevier.com/locate/ceramint

Microwave dielectric polymer-ceramics sintered at near room-temperature with moisture-proof ability

Guo-An Ding [a], Fei Liu [a,b,*], Jing-Jing Qu [a,c], Chang-Lai Yuan [d,**], Xiao Liu [d], Liu-Fang Meng [d], Guo-Hua Chen [d]

[a] School of Mechanical and Electrical Engineering, Guilin University of Electronic Technology, Guilin, 541004, PR China
[b] Guangxi Key Laboratory of Manufacturing System and Advanced Manufacturing Technology, Guilin University of Electronic Technology, Guilin, 541004, PR China
[c] Department of Science and Technology, Guilin University of Aerospace Technology, Guilin, 541004, PR China
[d] Guangxi Key Laboratory of Information Materials, Guilin University of Electronic Technology, Guilin, 541004, PR China

ARTICLE INFO

Keywords:
H_3BO_3-PE polymer-ceramics
Moisture-proof ability
Ultra-low temperature sintering
Microwave dielectric properties

ABSTRACT

(1-*x*)H_3BO_3-*x*PE (x = 0.0–0.5) microwave dielectric polymer-ceramics (composite ceramics) with ultra-low sintering temperatures (60–110 °C) were prepared via the traditional solid-state method to improve the moisture-proof ability of H_3BO_3 matrix ceramics. X-ray diffraction (XRD), back-scattered scanning electron microscopy (EDS-SEM), and Raman spectroscopy confirmed that H_3BO_3 and PE could coexist without intermediate phases. As the x value increased, the dielectric Q value and resonant frequency ($Q \times f$) decreased from 116,000 GHz (at 15.0 GHz) to 37,000 GHz (at 16.3 GHz), the relative permittivity (ε_r) varied between 2.83 and 2.14, and the temperature coefficient of the resonant frequency (τ_f) shifted from −147 ppm/°C to +27 ppm/°C in the (1-*x*)H_3BO_3-*x*PE ($0.0 \leq x \leq 0.5$) microwave ceramics at their optimal sintering temperatures. A near-zero τ_f value (+9 ppm/°C) was obtained in the 0.7H_3BO_3-0.3 PE composite, which simultaneously exhibited an ε_r value of ~2.38 and a $Q \times f$ value of ~46,000 GHz (at 15.7 GHz) after sintering at 100 °C for 1 h. Interestingly, through the hydrolysis experiment (24–384 h), the $Q \times f$ values of the 0.7H_3BO_3-0.3 PE and/or 0.6H_3BO_3-0.4 PE polymer-ceramics were basically maintained at approximately 35,000–40,000 GHz. These results showed that the novel (1-*x*)H_3BO_3-*x*PE polymer-ceramics should be the potential candidates for ultra-low temperature co-fired ceramic (ULTCC) technology.

1. Introduction

Microwave dielectric materials are made of resonators, antennas, filters and dielectric substrates which can be widely used in mobile communications, global satellite positioning and other modern communications technology [1–4]. In particular, microwave devices are required down to the millimeter scale with the high data transmission and low signal latency for the full arrival of the 5G era [5,6]. Therefore, to meet the requirements of the high integration and stability, the ultra-low temperature co-fired ceramic (ULTCC) technology has been received considerable attentions. At present, for the advanced substrate materials with the lower permittivity, numerous dielectric systems still need to be further modified. On the one hand, because the cheap electrode materials such as Ag and Al have lower melting points (<960 °C), the low permittivity microwave materials require an inherently low sintering temperature for co-firing with the electrode. On the other hand, a dielectric material with a lower permittivity ($\varepsilon_r < 3$), higher quality factor ($Q > 2000$ GHz), and good thermal stability ($\tau_f \sim 0$, temperature coefficient of resonant frequency) is essential for substrate materials in 5G microwave devices, but it is harder to obtain simultaneously these properties in the microwave frequency band. In these situations, it also should be noted that a lower Q value can lead to a greater loss of medium and affect the signal transmission and stability of microwave electronic components [7–14]. Thus, developing new microwave dielectric materials with the low permittivity, high Q value, and low sintering temperature is urgently required in these important materials research fields.

Microwave dielectric ceramics with acid salt series have gradually become a popular research topic. Especially, H_3BO_3 in borate is the most prominent and widely used as a sintering aid to prepare low-fired

* Corresponding author. School of Mechanical and Electrical Engineering, Guilin University of Electronic Technology, Guilin, 541004, PR China.
** Corresponding author. Guangxi Key Laboratory of Information Materials, Guilin University of Electronic Technology, Guilin, 541004, PR China.
E-mail addresses: liufeiguet@163.com (F. Liu), yclai-2002@163.com (C.-L. Yuan).

https://doi.org/10.1016/j.ceramint.2021.06.051
Received 29 March 2021; Received in revised form 27 May 2021; Accepted 4 June 2021
Available online 11 June 2021

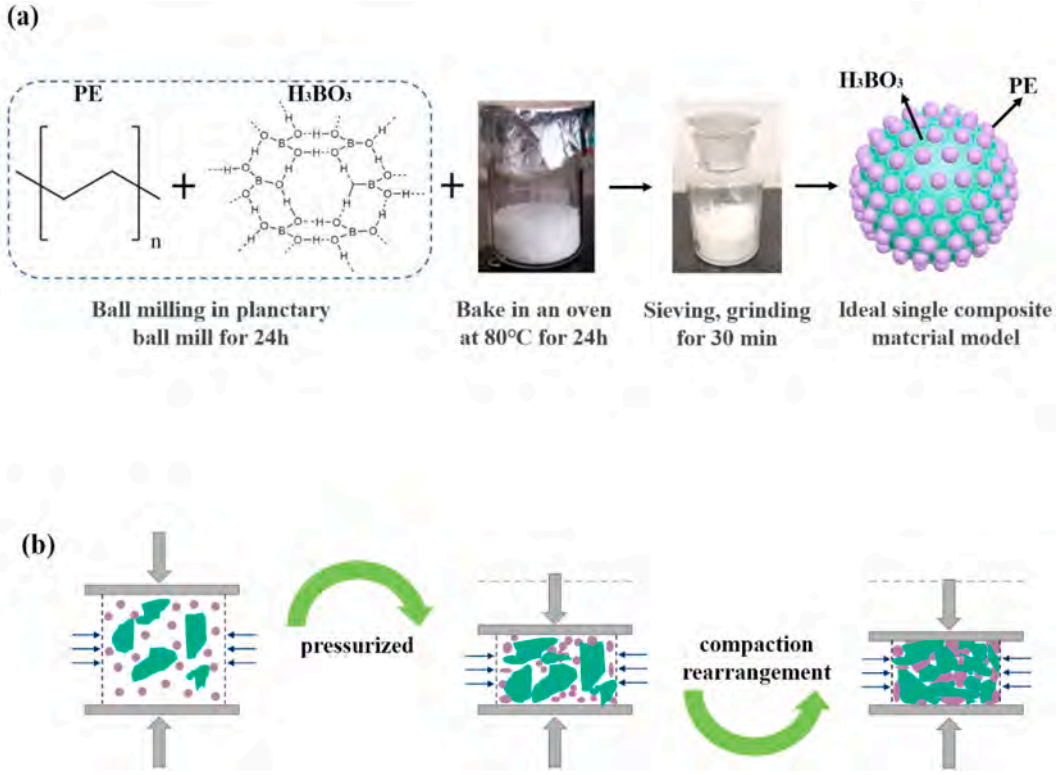

Fig. 1. Schematic diagrams of (a) raw powders synthesis and (b) pressing molding process for (1-x)H_3BO_3-xPE polymer-ceramics.

microwave dielectric ceramics [15–17]. Wang et al. used Li_2CO_3: Al_2O_3: H_3BO_3 = 1 : 1: 4 systems to prepare a series of microwave ceramics sintered below 750 °C, and these ceramics showed good dielectric properties ($\varepsilon_r \sim$ 3.2–3.9, $Q \times f \sim$ 21,500–35,500 GHz, $\tau_f \sim -52$ ppm/°C to −64 ppm/°C) and were co-fired with Ag [18]. Zhou et al. found that adding H_3BO_3 to Bi_2O_3 could acquire densely sintered ceramics below 650 °C and exhibited the favorable microwave dielectric properties with an ε_r value of ~12.14, a $Q \times f$ value of ~14,800 GHz, and a τ_f value of ~ −72 ppm/°C, achieving chemical compatibility with Al electrode co-firing [19]. Furthermore, a new CuO–ZnO–B_2O_3–Li_2O glass/Al_2O_3 ceramic composite was prepared by solid-state reaction method for ultra-low temperature co-firing ceramics (ULTCC), which was compatible with Ag and Al electrode co-firing at 640 °C [20]. Zhou et al. reported $LiBO_2$–H_3BO_3–B_2O_3–Li_2CO_3 microwave composite ceramics sintered at 640 °C with high-performance dielectric properties ($\varepsilon_r \sim$ 5.95, $Q \times f \sim$ 41,800 GHz, and $\tau_f \sim -72$ ppm/°C) [21]. Also, some studies have reported the dielectric properties of pure H_3BO_3 ceramics. Pang et al. obtained the new HBO_2 ceramics ($\varepsilon_r \sim 2.12 \pm 0.02$, $Q \times f \sim$ 32,700 ± 300 GHz, and $\tau_f \sim -43 \pm 3$ ppm/°C) by low temperature sintering and dehydration of being the H_3BO_3 ceramics at 190 °C, which provides the possibility for designing some new inorganic and organic composite functional materials to be applied in ULTCC technology for the future development [22]. In addition, Ding et al. obtained the densified H_3BO_3 ceramics with excellent microwave dielectric properties ($\varepsilon_r \sim$ 2.78–2.89, $Q \times f \sim$ 56,900–59,400 GHz, and $\tau_f \sim -91$ ppm/°C to −95.5 ppm/°C) by dry pressing powder at room temperature, and reported that the pressure and dwell time were key factors for densifying H_3BO_3 ceramics, in which the optimal pressure was approximately 384 MPa and the best holding time was approximately 300 s [23]. Li et al. reported that H_3BO_3 ceramics prepared by a simple cold sintering method had the higher relative density, more homogenous microstructures, and better microwave dielectric properties, with an ε_r value of ~2.84, a $Q \times f$ value of ~146,000 GHz, and a τ_f value of ~ −242 ppm/°C compared with those dry pressed at room temperature. Of note, the $Q \times f$ values of the pure H_3BO_3 ceramics decreased markedly from 146,000 GHz to 75,000 GHz after placing them in air for 24 h due to the fact that the H_3BO_3 ceramics extremely easily absorbed water, which was also a key problem to be urgently resolved in borate-based microwave ceramics systems [24]. In response to this point, by trying to combine the H_3BO_3 matrix ceramics with the polymer particles, it is quite possible that achieving a superior comprehensive performance judgment in a new polymer-ceramic system. Additionally, in many low loss polymer materials, PE has the relative good thermoplasticity, lower ε_r, and better moisture absorption resistance [25–27]. For example, Lin et al. prepared (PE/TiO_2) composite material with very low dielectric loss ($\tan\delta < 1.0 \times 10^{-3}$) by filling polyethylene PE with rutile phase TiO_2 by melt mixing method and thermal molding technology [28].

Based on the above mentioned reports and research, it is quite necessary to study the lower densification sintering temperatures and moisture-proof ability about the H_3BO_3 matrix ceramics. Thus, in this work, we prepared polymer-ceramics (composite ceramics) using H_3BO_3 and PE as matrix powders by the conventional solid-phase method in a temperature range of 60–110 °C. The relationship between the variations in the microstructures, phase composition and content, microwave dielectric characteristics, and moisture-proof ability of the H_3BO_3-PE polymer-ceramic systems were investigated and analyzed in detail as well.

2. Experimental procedure

(1-x)H_3BO_3-xPE (x = 0.0, 0.1, 0.2, 0.3, 0.4, and 0.5) microwave dielectric polymer-ceramic specimens were prepared by the solid-state reaction method. High-purity raw H_3BO_3 (≥99.5%, Xilong Chemical Reagent Co., Ltd, China) and PE (≥99.0%, Petro Chemical Co., Ltd, China) powders were used as starting materials. The H_3BO_3 powders were dried at 60 °C for 24 h to remove the absorbed moisture. The matrix materials were weighed in the appropriate mass ratio and mixed by grinding with ZrO_2 balls in ethanol media for 24 h. The resulting slurries were dried in an oven at 80 °C for 24 h, and the dried powders have been thoroughly sieved. The dried powders were directly

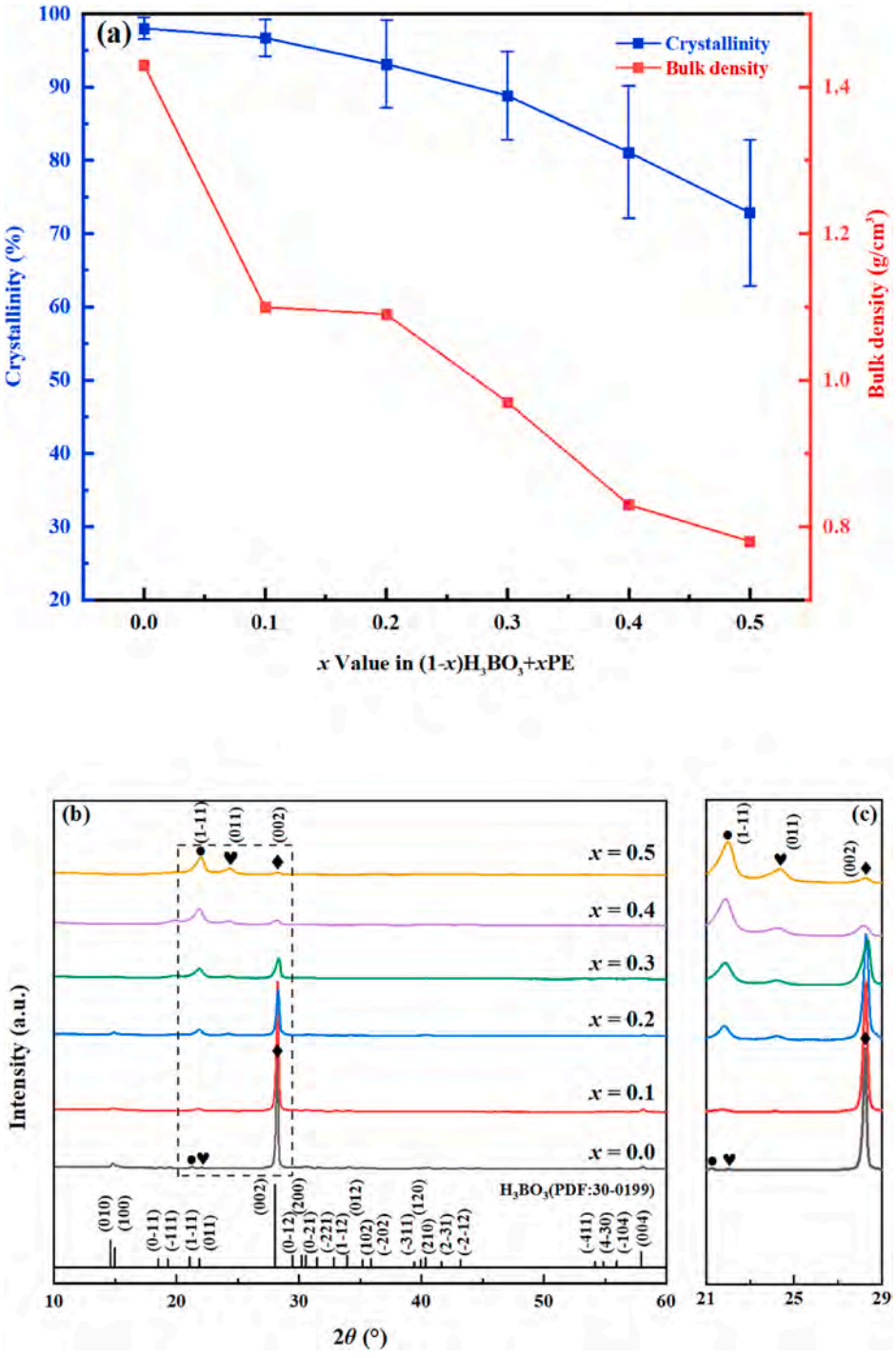

Fig. 2. (a) Bulk density and crystallinity, (b) room-temperature XRD patterns, and (c) the characteristic peaks of $2\theta = 21–29°$ of $(1\text{-}x)H_3BO_3$-xPE ($0.0 \leq x \leq 0.5$) polymer-ceramic samples sintered at their optimal temperatures.

uniaxially pressed by a manual tableting machine to form the H_3BO_3-PE cylindrical embryoid with a diameter of 12 mm and a height of 5–6 mm. The uniaxial pressure was approximately 20 MPa–512 MPa, and the dwell time was approximately 3–5 min. These compounded $(1\text{-}x)H_3BO_3$-xPE (x = 0.0–0.5) samples were sintered under given pressures at 60–110 °C for 1 h.

The bulk densities of the $(1\text{-}x)H_3BO_3$-xPE samples were measured using the geometric method. The phase compositions of the $(1\text{-}x)H_3BO_3$-xPE ceramics were analyzed by X-ray diffraction (XRD) using Cu-$K\alpha$ radiation (D8-Advance, Bruker, Germany) at room temperature in a 2θ range of 10–60°. The crystal structure of the ceramic samples was assessed in detail using Raman spectra observed by a Lab RAM HR Evolution (Horiba JY, France) Raman spectrometer. The microstructures of the surfaces, fractured surfaces, and elementary analysis were investigated by scanning electron microscopy (SEM, Model JSM6380LV, JEOL, Tokyo, Japan) equipped with energy disperse spectroscopy (EDS). The microwave dielectric properties of the ceramics were evaluated using a vector network analyzer (E5230C, Agilent, USA). Considering the influence of the alternating magnetic fields and errors caused by resistivity in parallel metal plates as the measurement of the lower relative permittivity [29,30], the ε_r and $Q \times f$ values were measured at approximately 14.5–17.0 GHz using the $TE_{01\delta}$ mode

dielectric resonator technique. Additionally, the τ_f values were evaluated at approximately 12.0–19.0 GHz by the Hakki-Coleman method using the following formula:

$$\tau_f = \frac{\Delta f_0}{f_0 \Delta T} = \frac{f_{75} - f_{25}}{f_{25} \times 50} \quad (2\text{–}1)$$

where f_{75} and f_{25} represent the resonant frequencies at 75 °C and 25 °C, respectively.

3. Results and discussion

Fig. 1(a) shows the synthesis process of the (1-x)H_3BO_3-xPE polymer-ceramic raw materials in detail. Through high-energy ball milling, PE and H_3BO_3 are mixed according to a certain mass ratio by ball milling. Fig. 1(a) displays the ideal state model, where the PE is uniformly attached to the surface of the H_3BO_3. During the drying process, the temperature environment is lower than the melting point of the H_3BO_3 and PE, respectively. The mixture can form a block, so the drying temperature point is set at 80 °C for this experiment. The density of ceramic samples is extremely important to the microwave dielectric properties. It has been reported in the literature that there are two mechanisms promoting the densification of ceramics during the near-room temperature sintering process [31,32]. The powders are compacted and rearranged by external forces, and the properties of the materials' matrix accelerate the mass transport through water as a transient liquid phase using the solution-precipitation mechanism. The densification molding process of the (1-x)H_3BO_3-xPE polymer-ceramics is shown in Fig. 1(b). Wherein, in these composite ceramics, the gap degree caused by the material characteristics of the H_3BO_3 and PE has a substantial impact on the denseness of the molded embryo, considering that the H_3BO_3 is a brittle deformation material and the PE is a plastic deformation material. Therefore, the H_3BO_3 is likely to rupture during the pressing process, while PE is deformed plastically due to the force. In view of this, the following equation is proposed [33]:

$$\sigma = \sigma_0 e^{-BP} \quad (3\text{–}1)$$

where σ is the density of the molded embryo, σ_0 is the density of the molded embryo with zero gap in the ideal state, B is a constant, and P is the gap degree, respectively. Uniaxial pressurization induces a relative motion between the H_3BO_3 and PE materials, while the mold wall also reveals the reverse extrusion pressure on the powder to fill the gaps. As the pressure increases to the maximum and enters the holding state, the PE powders deform and fill the gaps between the broken H_3BO_3 and other blank positions. The (1-x)H_3BO_3-xPE polymer-ceramic powders enter the compaction and rearrangement stage, the gap degree therefore reaches the minimum state and forms a dense embryo.

Fig. 2(a) illustrates the bulk density and crystallinity of the (1-x)H_3BO_3-xPE ($0.0 \le x \le 0.5$) polymer-ceramics at their optimum sintering temperatures. As the increased x value, the bulk density of the (1-x)H_3BO_3-xPE ceramics decreases from approximately 1.43 g/cm^3 at x = 0.0 to approximately 0.78 g/cm^3 at x = 0.5, and then shows a continuous declining trend. This indicates that a large amount of the PE introduced into the H_3BO_3 matrix can increase the porosity and affect the microwave dielectric properties of the composite materials. The crystallinity of the composite ceramic specimens decreases from ~98.01% to ~72.83% by means of the simple peak fitting in XRD analysis software. Fig. 2(b) shows the typical XRD patterns of the (1-x)H_3BO_3-xPE ($0.0 \le x \le 0.5$) polymer-ceramics at room temperature sintered at the optimum sintering temperatures. The vast majority of the diffraction peaks in the samples can be corresponded to the triclinic H_3BO_3 (PDF#30–0199), but the changes in the position and intensity of the main peaks between the ceramics and raw powders (as shown at the bottom of Fig. 2(b)) can also be observed as the gradually increased x value, indicating that the specimen's matrix is still a ceramic material while the crystal structures of the (1-x)H_3BO_3-xPE composite ceramics

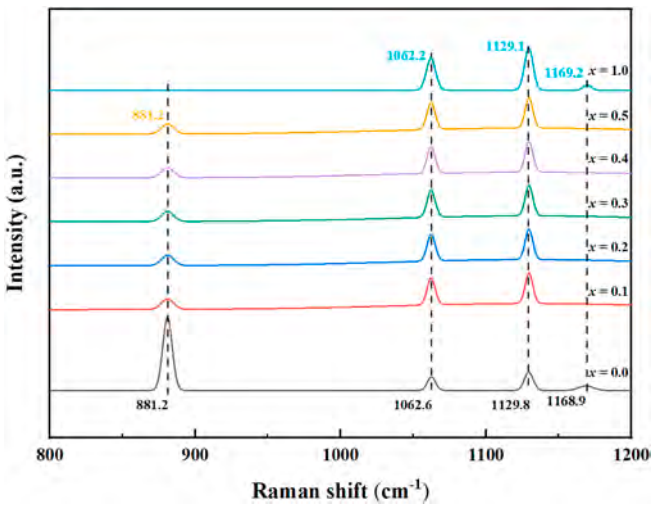

Fig. 3. Room-temperature Raman spectra of the (1-x)H_3BO_3-xPE ($0.0 \le x \le 0.5$, $x = 1.0$) samples sintered at their optimal temperatures.

are affected by the increase of the PE doping in the investigated components range of x = 0.0–0.5. Fig. 2(c) clearly shows that the (1–11), (011), and (002) diffraction peaks of the (1-x)H_3BO_3-xPE polymer-ceramics gradually change, and the main peak of the x = 0.1 sample is appeared at (002), which matches that of the H_3BO_3, but the peak intensity is stronger than that in the pure H_3BO_3. When $x > 0.1$, the main peak (002) is weaker gradually, while the (1–11) and (011) peaks gradually strengthen. As the x value further increases, both positions shifted to the higher 2θ and the (1–11) peak intensity become the most prominent due to the gradual decrease in the crystallinity of the (1-x)H_3BO_3-xPE (x = 0.0–0.5) polymer-ceramics, consistent with those shown in Fig. 2(a).

Raman spectroscopy is a valuable tool to study the phase transition of organic/inorganic composites. Increasing or decreasing the Raman mode and Raman peak displacement is an important basis for evaluating the crystal phase transition of microwave dielectric ceramic materials [34,35]. According to the group theory analysis method and the orthogonality of characteristic criterion, there are 28 different vibration modes of H_3BO_3 phase, given as follows:

$$\Gamma_{H_3BO_3} = 4A_g + 3B_g + 2E_{1g} + 5E_{2g} + 3A_u + 4B_u + 5E_{1u} + 2E_{2u} \quad (3\text{–}2)$$

where A_g (E_{1g}), E_{2g}, A_u, E_{1u}, and B_g (B_u, E_{2u}) are Raman active, IR inactive, IR active, Raman inactive, neither Raman active nor infrared active, respectively [36]. Consequently, H_3BO_3 crystal has 18 Raman active modes and 10 IR active modes. Based on these theories, the Raman spectrum of (1-x)H_3BO_3-xPE ($0.0 \le x \le 0.5$, $x = 1.0$) samples in bands 800-1200 cm^{-1} is shown in Fig. 3 in detail. For the Raman behaviors of the pure H_3BO_3 sample ($x = 0.0$) and PE sample ($x = 1.0$), the most remarkable point is that both these two pure content have peaks at 1062-1063 cm^{-1}, 1129-1130 cm^{-1}, and 1168-1170 cm^{-1}, and their positions are very close, which also explains why these (1-x) H_3BO_3-xPE (x = 0.0–0.5) composite materials can maintain a ceramic material matrix even as the x value increases to 0.5. Besides, there is almost no movement in the peak of the (1-x)H_3BO_3-xPE ceramic samples in the 881.2 cm^{-1} band as the PE increases ($x = 0.0$–0.5), and only this Raman peak's intensity is weakened. In addition, the peak intensities from x = 0.1 to x = 0.5 gradually increase in the bands at approximately 1062–1063 cm^{-1} and 1129-1130 cm^{-1}, but they are lower than those of the pure PE in this band. As a result, it can be inferred from the variations in the peak intensities of the Raman spectra that the PE polymer and H_3BO_3 ceramic phase can be coexistent without other second and/or intermediate phases, which is consistent with XRD analysis results.

SEM images of the polished and thermally etched cross-sections of

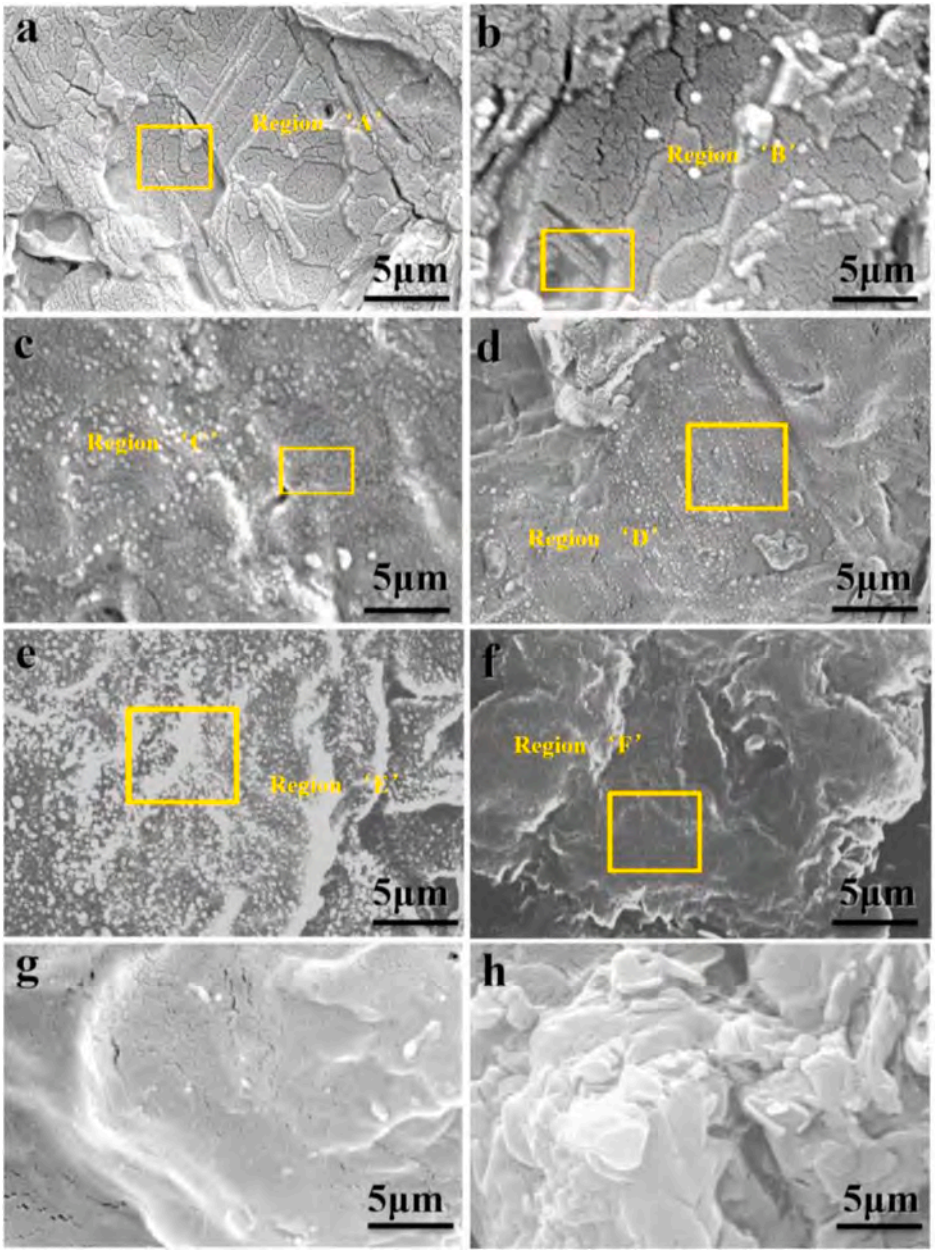

Fig. 4. SEM micrographs of (1-x)H_3BO_3-xPE ($0.0 \leq x \leq 0.5$) polymer-ceramics sintered at 100 °C for 1 h: (a) $x = 0.0$, (b) $x = 0.1$, (c) $x = 0.2$, (d) $x = 0.3$, (e) $x = 0.4$, and (f) $x = 0.5$, correspond to the surfaces; and (g) $x = 0.4$ and (h) $x = 0.2$, correspond to the fractured surfaces.

the (1-x)H_3BO_3-xPE ($0.0 \leq x \leq 0.5$) polymer-ceramics sintered at 100 °C for 1 h are shown in Fig. 4. In accordance with Fig. 4(a)-4(f), the porosity increases as the increase of the x value at the same sintering temperature, and an increasing number of PE polymers are attached to the surface of the matrix and show the uniform dispersion, which means that the PE content has a significant influence on the microstructures, sintering behaviors, and moisture-proof abilities for the H_3BO_3 ceramics. By comparing Fig. 4(a) and (b), it is obvious that there are some small white dots scattered in the $x = 0.1$ sample, and the dots should be the PE polymers (PE melting point > 100 °C [37]). As shown in Fig. 4(c), the local small white spots aggregate and the pores increase at $x = 0.2$ specimen. However, there are a few pores with the $x = 0.3$ sample as shown in Fig. 4(d), and the distribution of the PE on the surface of the H_3BO_3 is relative uniform and regular. As shown in Fig. 4(e), the distribution of the PE on the surface of the $x = 0.4$ sample is more uniform and compact due to the further increase in the PE doping. For the $x = 0.5$ sample presented in Fig. 4(f), the PE content is more prominent and integrated into the H_3BO_3 matrix. To further observe the internal microstructures, the $x = 0.2$ and $x = 0.4$ samples are selected to observe and survey the fractured surfaces. In comparison, the pores of the $x = 0.4$ sample seen in Fig. 4(g) are much smaller than those of the $x = 0.2$ sample, shown in Fig. 4(h), while the grains are larger and more obvious at $x = 0.2$. The distribution of the PE polymer shown in Fig. 4(g) is greater than that shown in Fig. 4(h) in the (1-x) H_3BO_3-xPE polymer-ceramics, which is exactly the reason why a certain amount of PE-doping can effectively improve the moisture-proof ability of H3BO3 matrix.

To further investigate the phase composition and element content of (1-x)H_3BO_3-xPE ($0.0 \leq x \leq 0.5$) polymer-ceramic specimens, energy-dispersive spectroscopy (EDS) is used to analyze the grains on the surface of the sample as demonstrated in regions 'A'-'F' corresponding to Fig. 4(a), (b), 4(c), 4(d), 4(e), and 2(f), respectively. EDS graphs and data on the (1-x)H_3BO_3-xPE samples are shown in Fig. 5(a)-5(f). According to the EDS analysis results of region 'A' selected randomly from Fig. 4(a),

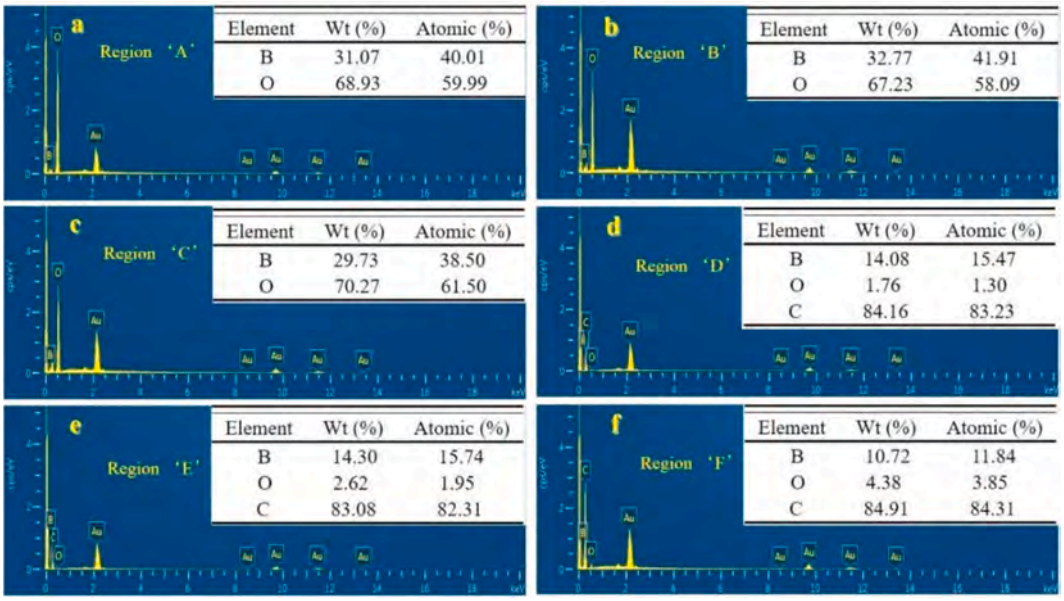

Fig. 5. EDS graphs and data of (a) region 'A', (b) region 'B', (c) region 'C', (d) region 'D', (e) region 'E', and (f) region 'F' from the samples' surfaces in Fig. 4(a), (b), 4 (c), 4(d), 4(e), and 4(f) respectively of (1-*x*)H_3BO_3-*x*PE ($0.0 \leq x \leq 0.5$) polymer-ceramics sintered at 100 °C for 1 h.

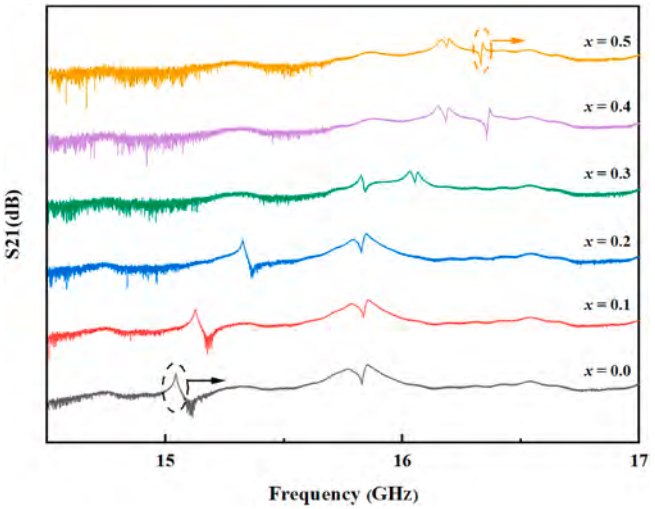

Fig. 6. Resonant peak of (1-*x*)H_3BO_3-*x*PE ($0.0 \leq x \leq 0.5$) microwave materials at their optimal sintering temperatures.

the atomic ratio of B and O is approximately to 2 : 3 (seen Fig. 5(a)), but it can also be speculated that the main matrix phase grains are belonged to H_3BO_3 on account of the fact that H element can not be quantitatively detected, combined with the above analysis. In the regions 'B' and 'C' corresponding to the $x = 0.1$ and $x = 0.2$ samples from the EDS data shown in Fig. 5(b) and (c), there is almost no C element detected in these regions, indicating that the PE distribution of the $x = 0.1$ and $x = 0.2$ composite ceramics is more concentrated or sporadically distributed. As shown in the EDS data in Fig. 5(d)-5(f), the PE doping amount increases between $x = 0.3$ and $x = 0.5$, resulted in the rapidly increasing C element content. These three components ($x = 0.3$–0.5) of the C element content is very close, meanwhile, the mass ratio in the B, C and O elements and the atomic percentage changes are almost the same as well. These results can further explain that the surfaces of the composite ceramics at $x = 0.4$ and 0.5 are almost compact and have a uniform distribution, combined with the XRD patterns and Raman spectra analyses.

Fig. 6 shows the resonant peak evolution diagram of the (1-*x*)H_3BO_3-*x*PE ($0.0 \leq x \leq 0.5$) microwave polymer-ceramics at their optimal sintering temperatures measured at the resonant cavity method under a vector network analyzer. In the $TE_{01\delta}$ mode, the equation is shown in the following [38]:

$$f_0 \approx \frac{c}{D\sqrt{\varepsilon_r}} \tag{3-3}$$

where c is the speed of light, f_0 is frequency, D is approximately the diameter of the resonating body, and ε_r is the dielectric constant of composite materials. The resonant frequency of composites is inversely proportional to the dielectric constant. In the pure H_3BO_3 ceramics, the resonance peak is approximately 15.0 GHz. As the PE content increases, the sample's resonance peak gradually shifts to the high frequency direction. When $x = 0.5$, the ceramic's resonance peak moves to approximately 16.3 GHz, indicating that the peak shape maintenance and directional movement ensure the accuracy of the measurement of the microwave dielectric properties.

Fig. 7 shows the microwave dielectric properties in the (1-*x*)H3BO3-*x*PE ($x = 0.0$–0.5) polymer-ceramic samples sintering at their optimal densification temperatures, and other sintering temperatures and dielectric characteristics (ε_r and $Q \times f$ values) of the (1-*x*)H3BO3-*x*PE ($x = 0.0$–0.5) specimens are listed in Table 1. Wherein, all the samples are sintered below 110 °C, and the pure H3BO3 ceramics are densely formed at near room-temperature, which is also reported by Li et al. in Ref. [24]. The ε_r values of dielectric ceramic materials are usually influenced by many factors, including in the crystallinity, ionic polarizability, secondary phase, and degree of densification [39–41]. In this work, the ε_r value of the composite ceramic decreases from ~2.83 ($x = 0.0$) to ~2.14 ($x = 0.5$) as the x value increases in the optimal densification temperatures. The H_3BO_3 ceramic is composed of PE by dry pressing and cold sintering to produce H_3BO_3-PE polymer-ceramic in the absence of chemical reactions between the phases. Therefore, the PE is introduced into the ceramic matrix as its own body without crystallization and still being an amorphous phase, resulting in the lower permittivity and density in these material systems. In addition, two dielectrics with different ε_r values can be combined to obtain a solid solution or composite material with the desired properties. According to Lichtenecker's logarithmic rule, it can describe the interaction relationship between two components, and predicts the performance of products correlated with the volume fraction (x and 1-x) and relative permittivity coefficients (ε_1 and ε_2) to the final relative permittivity ε by Eqs. (3–4) [42,

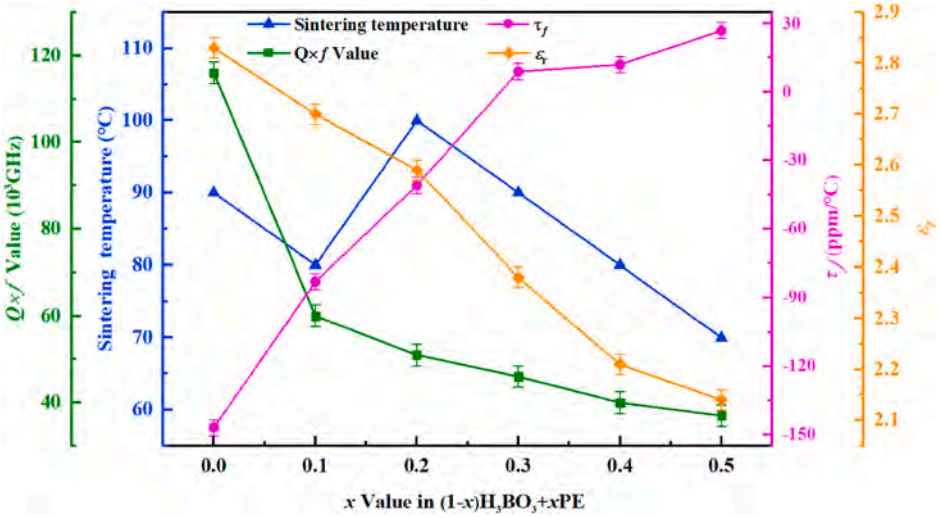

Fig. 7. The relatively optimal densification sintering temperature of the microwave dielectric properties (ε_r, $Q \times f$, and τ_f values) in the (1-x) H_3BO_3-xPE (x = 0.0–0.5) polymer-ceramic samples as a function of the x value.

Table 1
ε_r and $Q \times f$ values of the (1-x)H_3BO_3-xPE (x = 0.0–0.5) specimens at different sintering temperature.

x value	Sintering temperature (°C)	f_0 (GHz)	$Q \times f$ (GHz)	ε_r	tanδ
0.0	60	14.94	89500	2.83	0.000167
0.0	70	14.98	85600	2.81	0.000175
0.0	80	14.93	105900	2.84	0.000141
0.0	90	14.97	115700	2.83	0.000128
0.0	100	14.95	88500	2.83	0.000169
0.0	110	14.95	88400	2.83	0.000169
0.1	60	15.08	58900	2.66	0.000256
0.1	70	15.09	56700	2.66	0.000266
0.1	80	15.03	59600	2.70	0.000252
0.1	90	15.02	58200	2.69	0.000258
0.1	100	15.03	47900	2.70	0.000314
0.1	110	15.06	46900	2.68	0.000321
0.2	60	15.22	46100	2.58	0.000330
0.2	70	15.23	49600	2.58	0.000307
0.2	80	15.21	44200	2.59	0.000344
0.2	90	15.17	39500	2.58	0.000384
0.2	100	15.26	50600	2.59	0.000300
0.2	110	15.22	40300	2.58	0.000378
0.3	60	15.52	39700	2.39	0.000391
0.3	70	15.52	41400	2.38	0.000375
0.3	80	15.65	34300	2.30	0.000456
0.3	90	15.66	46100	2.38	0.000340
0.3	100	15.59	39700	2.35	0.000393
0.3	110	15.62	39500	2.34	0.000395
0.4	60	16.18	25900	2.16	0.000625
0.4	70	16.19	30300	2.15	0.000534
0.4	80	16.16	39800	2.21	0.000406
0.4	90	16.16	36400	2.22	0.000444
0.4	100	16.21	35200	2.13	0.000461
0.4	110	16.22	27600	2.13	0.000587
0.5	60	16.19	35300	2.16	0.000459
0.5	70	16.28	37100	2.14	0.000437
0.5	80	16.17	20100	2.19	0.000805
0.5	90	16.16	9500	2.12	0.00170
0.5	100	16.14	14200	2.16	0.00114
0.5	110	16.20	26200	2.14	0.000619

43]:

$$\log \varepsilon = (1-x)\log \varepsilon_1 + x \log \varepsilon_2 \quad (3\text{–}4)$$

Therefore, the continuous addition of PE macromolecules with lower ε_r to H_3BO_3 makes the dielectric constant of the H_3BO_3-PE microwave materials decrease gradually. Furthermore, for the quality factor (Q), it is well known that the increasing porosity can lead to the incremental dielectric loss in microwave dielectric ceramics [44], In this study, the increasing porosity and decreasing the bulk density from ~1.43 g/cm^3 to ~ 0.78 g/cm^3 in the (1-x)H_3BO_3-xPE ($0.0 \leq x \leq 0.5$) polymer-ceramics are mainly reasons for the significant decrease in the $Q \times f$ values from approximately 116,000 GHz to approximately 37,000 GHz consistent with Fig. 4 and 2(a). Moreover, the pursuit of near-zero τ_f values has always been an important criterion for judging the dielectric properties of microwave ceramics. For composite ceramics, the common method is combining the positive τ_f value material with a negative τ_f value material to achieve zero-value adjustment [45]. In the (1-x)H_3BO_3-xPE polymer-ceramic systems sintered at the optimal densification temperatures, the τ_f value displays an upward trend from approximately −147 ppm/°C (x = 0.0) to approximately +27 ppm/°C (x = 0.5), and the τ_f values are calculated using the mixing rule shown in Eqs. (3–5):

$$\tau_f = \sum_{i=1}^{n} v_i \tau_{fi} \quad (3\text{–}5)$$

where v_i and τ_{fi} are the volume fraction and temperature coefficient of the resonant frequency of the ith phase, respectively. The 0.7H_3BO_3-0.3 PE sample sintered at 90 °C for 1 h possesses the optimal microwave dielectric properties of ε_r ~2.38, $Q \times f$ ~46,000 GHz and near-zero τ_f ~ +9 ppm/°C.

The $Q \times f$ value of microwave dielectric materials is sensitive to the absorbed moisture, and has been therefore measured as a function of the exposure time to evaluate the moisture resistance of the (1-x)H_3BO_3-xPE polymer-ceramics via hydrolysis experiments. Fig. 8(a) shows the apparent morphology of the ceramic samples with x = 0.0, 0.3, and 0.4 through the hydrolysis experiment. The x = 0.0 sample is intact but the powder is hydrolyzed after the experiment. Also, the hydrolysis experiment continues as time goes on, the sample will be hydrolyzed into powder from the block. As the x value increases to 0.3, some cracks emerge in the specimen during the hydrolysis experiment, while there is without the separation of the powders from the polymer-ceramics after the water absorption, indicating that the PE doping can effectively prevent the water absorption of the H_3BO_3 to a certain extent. Furthermore, the x = 0.4 composite ceramic sample retains its integrity after the hydrolysis experiments, further proving that a certain amount of PE can reduce the water absorption capacity of the (1-x)H_3BO_3-xPE polymer-ceramic systems. Fig. 8(b) and (c) show the changes in the $Q \times f$ values and mass of the three content samples of x = 0.0, x = 0.3, and x = 0.4 during the hydrolysis experiments. When x = 0.0, the $Q \times f$ value

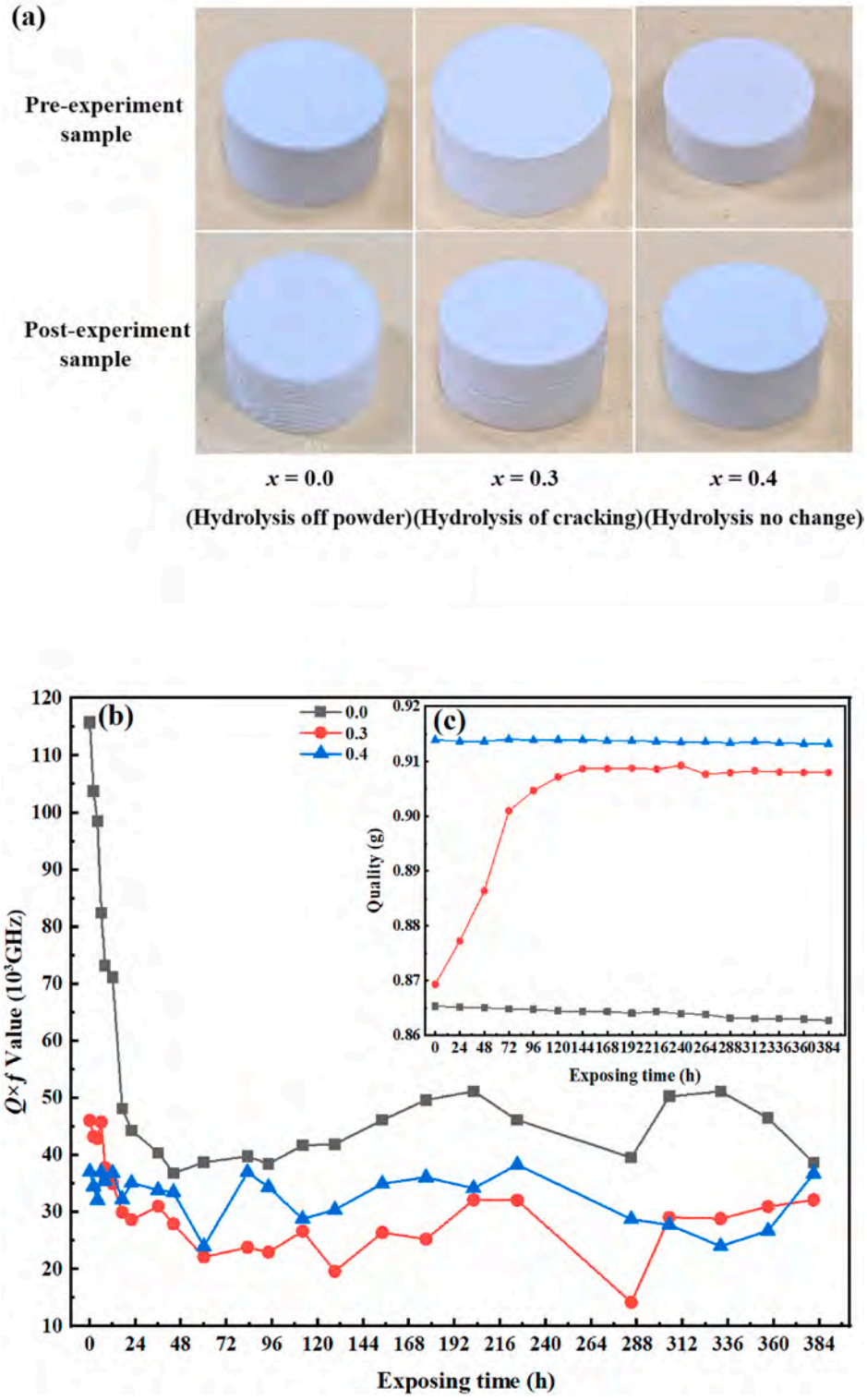

Fig. 8. (1-x)H_3BO_3-xPE (x = 0.0, 0.3, and 0.4) samples with (a) the comparison of the changes before and after hydrolysis experiment; the variation rule of (b) $Q \times f$ value and (c) mass of the samples with exposing time during the hydrolysis experiment.

decreases rapidly from an initial value of approximately 116,000 GHz to approximately 48,000 GHz during in the first 17 h, while it continually decreases to approximately 40,300 GHz over the next 36 h. As the exposure time increases to 384 h, the $Q \times f$ value is not decreased significantly, and fluctuates between ~39,000 GHz and ~50,000 GHz, and the ceramic sample's quality decreases gradually. Combined with the hydrolysis experiments in the $x = 0.0$ sample shown in Fig. 8(a), it is clear that the ceramic's $Q \times f$ value continues to deteriorate when it is exposed to a humid environment for a longer time. Furthermore, as shown in Fig. 4(d) and Fig. 5(d), although the PE polymer is uniformly distributed on the surface of the H_3BO_3 matrix, there are many internal pores and a limited amount of PE content that are not arranged effectively and reasonably inside the matrix. As shown in Fig. 8(c), the ceramic with $x = 0.3$ in the water absorption reaches a saturation value

after 216 h. The mass increases from 0.85 g to 0.89 g, and then stabilizes at approximately 0.90–0.91 g. Fig. 8(b) shows a sharp decrease in the $Q \times f$ value (below 20,000 GHz) from 216 h to 288 h of exposure time, so 216 h is the final cracking time for the $x = 0.3$ sample. The ceramic at $x = 0.3$ is in a state of cracking, but the $Q \times f$ value fluctuates in a range of 20,000–35,000 GHz in most instances. It is worth noting that there is no obvious change in the appearance, $Q \times f$ value, and quality for the $x = 0.4$ sample, and the fluctuating $Q \times f$ values are always approximately 40,000 GHz. Contrary to the hydrolyzation experiments, it is obvious that the $Q \times f$ values in the $x = 0.3$ and $x = 0.4$ polymer ceramics are not as high as the decreasing degree in the sample at $x = 0.0$, which indicates that the PE doping can effectively improves the H_3BO_3 moisture-proof ability and maintains some good dielectric properties to a certain extent.

4. Conclusion

(1-x)H_3BO_3-xPE (x = 0.0–0.5) polymer-ceramics were prepared using the traditional solid-state method. The XRD patterns and Raman analysis results indicated that the polymer-ceramics had two coexisting phases with a mainly ceramic matrix. The bulk densities of the polymer-ceramics displayed a decreasing trend. Using SEM observations of the polymer-ceramic's surface morphology, it was found that as the PE doping amount increased from $x = 0.0$ to $x = 0.5$, the pores of polymer-ceramics gradually increased, which was the primary reason for the decrease in the density. In the EDS analysis, the PE content was gradually uniformly attached to the surface of the H_3BO_3 matrix. From the measurement of microwave dielectric properties, the relative permittivity (ε_r) maintained a downward trend, and the temperature coefficient of the resonant frequency (τ_f) could be achieved a near-zero value by adjusting the PE content. Although there was a certain decrease in the dielectric Q value and resonant frequency ($Q \times f$), it still maintained about 37,000–50,000 GHz. The optimal microwave dielectric properties of $\varepsilon_r \sim 2.38$, $Q \times f \sim 46{,}000$ GHz (at 15.7 GHz) and $\tau_f \sim +9$ ppm/°C were obtained in the 0.7H_3BO_3-0.3 PE polymer-ceramic sintered at 100 °C for 1 h. Through the hydrolysis experiment conducted for more than 384 h, the pure H_3BO_3 ceramics appeared to hydrolyze and drop powder, and there were some cracks in the 0.7H_3BO_3-0.3 PE sample, but the 0.6H_3BO_3-0.4 PE sample was intact, and the $Q \times f$ values at $x = 0.4$ content could still be maintained at approximately 40,000 GHz. In future studies, we will introduce other polymer materials, such as PP, PFA, PET, PTFE, and PMMA, into a H_3BO_3 matrix to further evaluate the microwave dielectric properties, compactness, and moisture-proof abilities of H_3BO_3-based polymer-ceramic systems.

Declaration of competing interest

The authors declare that they have no known competing financial interests or personal relationships that could have appeared to influence the work reported in this paper.

Acknowledgement

Financial supports of the National Natural Science Foundation of China (Grants No. 61801135), the Natural Science Foundation of Guangxi Province, China (Grants No. 2018GXNSFBA281001), the Innovation Project of Guangxi Graduate Education, China (Grants No. YCBZ2020060), the Guangxi Key Laboratory of Manufacturing System & Advanced Manufacturing Technology (Grants No. 20-065-40-001z) and the Science and Technology Project of Guangxi Province, China (Grant No. 201819074 or 18281049) are gratefully acknowledged by the authors.

References

[1] I.M. Reaney, D. Iddles, Microwave dielectric ceramics for resonators and filters in mobile phone networks, J. Am. Ceram. Soc. 89 (7) (2006) 2063–2072.
[2] F. Liu, J.J. Qu, H.G. Yan, C.L. Yuan, T.T. Wei, G.H. Chen, L.F. Meng, H.W. Ning, Study on phase structures and compositions, microstructures, and dielectric characteristics of (1-x)$NdGaO_3$-$xBi_{0.5}Na_{0.5}TiO_3$ microwave ceramic systems, Ceram. Int. 46 (10) (2020) 16185–16195.
[3] D. Zhou, L.X. Pang, D.W. Wang, C. Li, B.B. Jin, I.M. Reaney, High permittivity and low loss microwave dielectrics suitable for 5G resonators and low temperature co-fired ceramic architecture, J. Mater. Chem. C. 5 (38) (2017) 10094–10098.
[4] L.X. Pang, D. Zhou, Modification of $NdNbO_4$ microwave dielectric ceramic by Bi substitutions, J. Am. Ceram. Soc. 102 (5) (2019) 2278–2282.
[5] I. Hameed, S.Y. Wu, L. Li, X.Q. Liu, X.M. Chen, Structure and microwave dielectric characteristics of $Sr_2[Ti_{1-x}(Al_{0.5}Nb_{0.5})_x]O_4 (x \leq 0.50)$ ceramics, J. Am. Ceram. Soc. 102 (10) (2019) 6137–6146.
[6] Z.X. Wang, C.L. Yuan, B.H. Zhu, Q. Feng, F. Liu, L. Miao, C.R. Zhou, C.H. Chen, Microwave dielectric properties of $Bi(Sc_{1/3}Mo_{2/3})O_4$ ceramics for LTCC applications, J. Mater. Sci. Mater. Electron. 29 (3) (2018) 1817–1822.
[7] W. Lei, Z.Y. Zou, Z.H. Chen, B. Ullah, A. Zeb, X.K. Lan, W.Z. Lu, G.F. Fan, X. H. Wang, X.C. Wang, Controllable τ_f value of barium silicate microwave dielectric ceramics with different Ba/Si ratios, J. Am. Ceram. Soc. 101 (1) (2018) 25–30.
[8] L.F. Meng, C.L. Yuan, B.H. Zhu, X. Liu, F. Liu, J.W. Xu, C.R. Zhou, G.H. Chen, Microwave dielectric properties of $Na_5RE(MoO_4)_4$ (RE = La, Gd, Dy, Er) ceramics with a low sintering temperature, J. Electron. Mater. 48 (1) (2019) 656–661.
[9] L. Li, W.B. Hong, X.J. Yan, X.M. Chen, Preparation and microwave dielectric properties of B_2O_3 bulk, Int. J. Appl. Ceram. Technol. 16 (5) (2019) 2047–2052.
[10] L. Li, W.B. Hong, G.Y. Chen, X.M. Chen, High-performance (1-x) ($0.2B_2O_3$-$0.8SiO_2$)-$xTiO_2$ (x = 0.025-0.1) glass matrix composites for microwave substrate applications, J. Alloys Compd. 774 (2019) 706–709.
[11] S.Z. Hao, D. Zhou, F. Hussain, W.F. Liu, J.Z. Su, D.W. Wang, Q.P. Wang, Z.M. Qi, C. Singh, S. Trukhanov, Structure, spectral analysis and microwave dielectric properties of novel $x(NaBi)_{0.5}MoO_4$-(1-x)$Bi_{2/3}MoO_4$ (x = 0.2-0.8) ceramics with low sintering temperatures, J. Eur. Ceram. Soc. 40 (10) (2020) 3569–3576.
[12] D. Zhou, C.A. Randall, L.X. Pang, H. Wang, J. Guo, G.Q. Zhang, X.G. Wu, L. Shui, X. Yao, Microwave dielectric properties of Li_2WO_4 ceramic with ultra-Low sintering temperature, J. Am. Ceram. Soc. 94 (2) (2011) 348–350.
[13] B.J. Tao, W.F. Wang, H.Y. Liu, T.X. Du, H.T. Wu, C.F. Xing, D.Z. Wng, Y.P. Zhang, Low-temperature sintering LiF-doped $Li_4Mg_3[Ti_{0.6}(Mg_{1/3}Nb_{2/3})_{0.4}]_2O_9$ microwave dielectric ceramics for LTCC applications, Ceram. Int. 47 (2) (2021) 2584–2590.
[14] J.J. Zheng, Y.H. Liu, B.J. Tao, Q. Zhang, H.T. Wu, X.Y. Zhang, Crystal structure and optimised microwave dielectric properties of $Ce_2(Zr_{1-x}Ti_x)_3(MoO_4)_9$ solid solutions, Ceram. Int. 47 (4) (2021) 5624–5630.
[15] H.F. Zhou, X.B. Liu, X.L. Chen, L. Fang, Y.L. Wang, $ZnLi_{2/3}Ti_{4/3}O_4$: a new low loss spinel microwave dielectric ceramic, J. Eur. Ceram. Soc. 32 (2) (2012) 261–265.
[16] X.H. Ma, S.H. Kweon, M. Im, S. Nahm, Low-temperature sintering and microwave dielectric properties of B_2O_3-added ZnO-deficient Zn_2GeO_4 ceramics for advanced substrate application, J. Eur. Ceram. Soc. 38 (14) (2018) 4682–4688.
[17] Z.J. Wang, R. Freer, Low firing temperature zinc molybdate ceramics for dielectric and insulation applications, J. Eur. Ceram. Soc. 35 (11) (2015) 3033–3042.
[18] K.G. Wang, H.F. Zhou, X.B. Liu, W.D. Sun, X.L. Chen, H. Ruan, A lithium aluminium borate composite microwave dielectric ceramic with low permittivity, near-zero shrinkage, and low sintering temperature, J. Eur. Ceram. Soc. 39 (4) (2019) 1122–1126.
[19] K.G. Wang, T.T. Yin, H.F. Zhou, X.B. Liu, J.J. Deng, S.X. Li, C.M. Lu, X.L. Chen, Bismuth borate composite microwave ceramics synthesised by different ratios of H_3BO_3 for ULTCC technology, J. Eur. Ceram. Soc. 40 (2) (2020) 381–385.
[20] J. Xi, G.H. Chen, F. Liu, F. Shang, J.W. Xu, C.R. Zhou, C.L. Yuan, Synthesis, microstructure and characterization of ultra-low permittivity CuO-ZnO-B_2O_3-Li_2O glass/Al_2O_3 composites for ULTCC application, Ceram. Int. 45 (18) (2019) 24431–24436.
[21] D. Zhou, L.X. Pang, D.W. Wang, Z.M. Qi, I.M. Reaney, High quality factor, ultralow sintering temperature $Li_6B_4O_9$ microwave dielectric ceramics with ultralow density for antenna substrates, ACS Sustain. Chem. Eng. 6 (8) (2018) 11138–11143.
[22] L.X. Pang, D. Zhou, W.B. Li, Z.X. Yue, High quality microwave dielectric ceramic sintered at extreme-low temperature below 200° and co-firing with base metal, J. Eur. Ceram. Soc. 37 (9) (2019) 3073–3077.
[23] X.B. Ding, Y.J. Gu, Q. Li, B.H. Kim, Q.F. Wang, J.L. Huang, Room temperature densified H_3BO_3 microwave dielectric ceramics with ultra-low permittivity and high quality factor for dielectric substrate applications, Ceram. Int. 46 (9) (2020) 13225–13232.
[24] W.B. Hong, L. Li, H. Yan, S.Y. Wu, H.S. Yang, X.M. Chen, Room-temperature-densified H_3BO_3 microwave dielectric ceramics with ultra-low permittivity and ultra-high $Q \times f$ value, J. Mater. Sci. 6 (2) (2020) 233–239.
[25] M.T. Sebastian, H. Jantunen, Polymer-ceramic composites of 0-3 connectivity for circuits in Electronics: a review, Int. J. Appl. Ceram. Technol. 7 (4) (2010) 415–434.
[26] X.Y. Huang, Q.Q. Ke, C.N. Kim, H.F. Zhong, P. Wei, G.L. Wang, F. Liu, P.K. Jiang, Nonisothermal crystallization behavior and nucleation of LDPE/Al nano- and microcomposites, Polym. Eng. Sci. 47 (7) (2007) 1052–1061.
[27] A.J. Bur, Dielectric properties of polymers at microwave frequencies: a review, Polym. J. 26 (1985) 963–977.
[28] H.X. Lin, Z.Z. Weng, Z.X. Xiong, Preparation and microwave dielectric properties of polyethylene/TiO2 composites, J. Electron. Mater. 48 (10) (2019) 6771–6776.
[29] D. Kajfez, A. Gundavajhala, Measurement of material properties with a tunable resonant cavity, Electron. Lett. 29 (22) (1993) 1936–1937.
[30] B.W. Hakki, P.D. Coleman, A dielectric-resonator method of measuring inductive capacities in the millimeter wave range, IEEE Trans. Microw. Theor. Tech. 8 (4) (1960) 402–410.

[31] J. Guo, H.Z. Guo, A.L. Baker, M.T. Lanagan, E.R. Kupp, G.L. Messing, C.A. Randall, Cold sintering: a paradigm shift for processing and integration of ceramics, Angew. Chem. Int. Ed. 55 (38) (2016) 11457–11461.
[32] J. Guo, R. Floyd, S. Lowum, J.P. Maria, T.H.D. Beauvoir, J.H. Seo, C.A. Randall, Cold sintering: progress, challenges, and future opportunities, Annu. Rev. Mater. Res. 49 (1) (2019) 275–295.
[33] E. Ryshkewitch, Compression strength of porous sintered alumina and zirconia, J. Am. Ceram. Soc. 36 (2) (1953) 65–68.
[34] J.J. Qu, F. Liu, X. Wei, C.L. Yuan, X.Y. Liu, G.H. Chen, Q. Feng, X.- ray Diffraction, Dielectric, and Raman spectroscopy studies of $SrTiO_3$-based microwave ceramics, J. Electron. Mater. 45 (1) (2016) 715–721.
[35] S.Z. Hao, D. Zhou, F. Hussain, J.Z. Su, W.F. Liu, D.W. Wang, Q.P. Wang, Z.M. Qi, Novel scheelite-type $[Ca_{0.55}(Nd_{1-x}Bi_x)_{0.3}]$ $MoO_4(0.2 \leq x \leq 0.95)$ microwave dielectric ceramics with low sintering temperature, J. Am. Ceram. Soc. 103 (12) (2020) 7259–7266.
[36] R.R. Servoss, H.M. Clark, Vibrational spectra of normal and isotopically labeled boric acid, J. Chem. Phys. 26 (5) (1957) 1175–1178.
[37] Z.H. Xue, Q.Y. Li, W. Zhang, C.H. Lu, Preparation and properties of PE/EG thermal conductivity composites for melt deposition molding, Polym. Eng. Sci. 36 (9) (2020) 88–96.
[38] M.T. Sebastian, R. Ubic, H. Jantunen, Low-loss dielectric ceramic materials and their properties, Int. Mater. Rev. 60 (7) (2015) 392–412.
[39] L.X. Pang, G.B. Sun, D. Zhou, $Ln_2Mo_3O_{12}$ (Ln=La, Nd): a novel group of low loss microwave dielectric ceramics with low sintering temperature, Mater. Lett. 65 (2) (2011) 164–166.
[40] D.J. Joyner, D.M. Hercules, Chemical bonding and electronic structure of B_2O_3, H_3BO_3, and BN: an ESCA, Auger, SIMS, and SXS study, J. Chem. Phys. 72 (2) (1980) 1095–1108.
[41] X.K. Lan, J. Li, Z.Y. Zou, G.F. Fan, W.Z. Lu, W. Lei, Lattice structure analysis and optimised microwave dielectric properties of $LiAl_{1-x}(Zn_{0.5}Si_{0.5})_xO_2$ solid solutions, J. Eur. Ceram. Soc. 39 (7) (2019) 2360–2364.
[42] R. Freer, F. Azough, Microstructural engineering of microwave dielectric ceramics, J. Eur. Ceram. Soc. 28 (7) (2008) 1433–1441.
[43] Y.J. Gu, J.L. Huang, Y. Wang, D.M. Sun, Q. Li, F.L. Li, H. Xu, Low temperature firing of CaO-Li_2O-Sm_2O_3-TiO_2 ceramics with $BaCu(B_2O_5)$ addition, Solid State Commun. 149 (2009) 555–558.
[44] H.C. Xiang, C.C. Li, H.L. Jantunen, L. Fang, A. Hill, An ultra-low loss $CaMgGeO_4$ microwave dielectric ceramic and its chemical compatibility with silver electrodes for LTCC applications, ACS Sustain. Chem. Eng. 26 (6) (2018) 6458–6466.
[45] F. Liu, J.J. Qu, C.L. Yuan, G.H. Chen, Crystal structure and dielectric properties of a new Na_2O-Nd_2O_3-CeO_2 ceramic system at microwave frequencies, Mater. Res. Bull. 98 (16) (2018) 8–14.